Cavitation Characteristics on Flow with Multi Cavitation Sources

LI Yongmei, ZHANG Dong, WANG Yongsheng, B. Y. Baoligao and LI Zhongyi,
China Institute of Water Resources and Hydropower Research (IWHR),
A1 Fuxing Road, Beijing, 100038, CHINA

Abstract

The cavitation characteristics were analyzed in this paper for the flood relief mid-outlets of Baise Multipurpose dam project, on the basis of depressurized model test of 1:50 in a specially designed vacuum chamber. The results of test demonstrate that there exists relatively distinct cavitation cloud at the gate slots and outlet diffusion zones of spillways. Mutual disturbance of cavitation noise from two sources leads to the relationship curve becoming concave downward and the frequency spectrum sound pressure level decreasing correspondingly when η is close to η_m ($\eta/\eta_m = 1$). Its pattern is not in conformity with the general law. The discovery may have certain supplementation for the standard of judging the cavitation emergence.

1. General Description

Baise Multipurpose Dam Project (hereinafter referred to as the project) is located on the upper reach of Youjiang River. For the overflow dam block a compound energy dissipation pattern achieved by overflow spillway tail-flaring piers, mid-outlet drop and bottom flow stilling basin was adopted. There are four overflow spillways with tail-flaring piers. Each of the three middle piers accommodates a mid-outlet that runs through the dam body and has its centerline coincide with that of gate pier. Each mid-outlet has an operating radial gate at the end to control discharge. Figure 1 demonstrates the layout.

2. Test Equipment and Method

The depressurized model for mid-outlet was designed according to the similarity law of gravity at a scale of 1:50. This test was conducted in the large-scale vacuum chamber in IWHR. The chamber has superior air tightness. The vacuum level inside the chamber remains unchanged or slightly varied within one week under condition of saturated air-content in water. Water quality maintains clear since antirust spray coating was applied. The observation window is large enough to provide a wide field of vision and facilitate clear observation. Water circulation pump is driven by stepless continuous speed regulation motor and each pipe is equipped with an individual pump, thus rendering simple and reliable operation.

The whole test detecting system is completely provided with electronic measuring instruments, of which the multi-point pressure monitoring detecting system is our patent product. As the only reliable pressure measuring system that can be applied inside the vacuum chamber at present, it is capable of committing calibration and check measurement under condition of high vacuum. The flow measuring system consists of orifice plate flow meter, differential pressure transducer and computer, and has the same accuracy and stability as the weir-type flow meter. Noise frequency spectrum analytic apparatus from B&K of Denmark was utilized to monitor flow noise. Computer-aided devices help master smooth data acquisition and processing.

To conduct the cavitation test, the model shall have the same flow cavitation number as the corresponding point of the prototype besides following the gravity similarity law. Therefore, the vacuum level inside the vacuum chamber shall be controlled as follows:

$$\eta_m = 1-h_v / h_\alpha – H_\alpha / (L_r / h_\alpha) + H_v / (L_r / h_\alpha) \quad (1)$$

In which: η_m—simulating vacuum level;

h_v -- saturated vapor pressure of water in model;

H_v -- saturated vapor pressure of water in prototype;

h_α -- atmospheric pressure in lab room;

L_r -- model geometric scale;

H_α -- atmospheric pressure at the location of prototype, it can be approximately calculated using the following formula.

$$H_\alpha = h_\alpha - \nabla Z / 900 \ (mH_2O) \quad (2)$$

In which: ∇Z – elevation difference between model and prototype (m).

Within the temperature range of 10~30°C, H_v can be calculated with the following formula.

$$H_v = 0.077\times1.06^{tw} - 0.013 \text{ (m } H_2O) \quad (3)$$

In which: t_w – water temperature (°C).

During actual calculation, H_v being taken as equal to h_v will render enough accuracy.

The flow cavitation number of overflow spillway was calculated using the following formula:

$$\sigma = \frac{\frac{p}{\gamma} + \frac{p_\alpha}{\gamma} - \frac{p_v}{\gamma}}{\frac{v^2}{2g}} \quad (4)$$

In which: p – relative pressure at individual measuring point;

p_α -- atmospheric pressure;

p_v -- vapor pressure;

ν -- flow velocity at individual measuring point,

calculated with Bernoulli's equation if energy loss is not taken into account.

The noise at $\eta = 0.85\eta_m$ (in which: η -- vacuum level inside vacuum chamber; η_m – simulated vacuum level) was taken as background noise. Whether cavitation occurs or not can be judged based on the noise frequency spectrum, sound pressure level increment (ΔSPL) and the variation processes of relative noise energy (E'/E_1). "E'" refers to the instantaneous noise energy at 10kHz or above, "E_1" the background time-average noise energy at this frequency band, and "E" the time-average noise energy at 10kHz or above. Based on the $E'/E_1 \sim \eta/\eta_m$ relationship curve, the development situation of cavitation in water flow can be further analyzed more intensively.

The cavitation safety factor (K) is calculated with the following formula:

$$K = \frac{\sigma}{\sigma_i} = \left[\frac{p/L_r + (1-\eta_m)p_\alpha - p_v}{\rho v^2/2}\right] / \left[\frac{p/L_r + (1-\eta_i)p_\alpha - p_v}{\rho v_i^2/2}\right] \quad (5)$$

In which: σ -- flow cavitation number of any point;

σ_i -- incipient cavitation number of this point;

P/L_r – pressure at this point of model;

L_r – geometrical model scale;

P_a – atmospheric pressure;

P_v -- vapor pressure;

ν -- flow velocity at this point;

ν_i -- flow velocity at this point in case of incipient cavitation, for the same point, $\nu = \nu_i$

3. Cavitation Test Results of Mid-outlet

The preliminary analysis of mid-outlet configuration demonstrates that cavitation likely occurs at the inlet, gate slot and exit diffusion section of mid-outlet. So hydrophones No.4 and No.5 were respectively set at the exit diffusion section (point A) and the inlet adjacent to the gate slot (point B), in order to monitor the cavitation behavior of water flow through mid-outlet. For the locations of hydrophones please refer to Figure 1. A piezometric hole was set on the left side of mid-outlet gate shaft in order to measure the water depth at gate shaft, with reference to Figure 1. The water depth at gate shaft is variable under various operating conditions. According to the reference (Li Zhongyi (1997)), the water depth at gate shaft can be calculated using the following formula:

$$H_w = H-\varphi^2\varepsilon^2(a/a_1)^2(H-\varepsilon a)(\alpha_1+\zeta_{in}+0.5\zeta_g) \quad (6)$$

In which: H_w – water depth above floor slab at gate shaft of mid-outlet;

H – water head above mid-outlet bottom;

a – height of mid-outlet opening at exit;

a_1 -- height of mid-outlet opening at gate slot;

α_1 – energy correction factor at gate slot;

ζ_{in} – local resistance loss factor at inlet;

ζ_g – resistance loss factor at gate slot;

ε -- flow constriction factor at exit;

φ -- flow velocity factor, which can be calculated using the following formula:

$$\varphi = \frac{1}{\sqrt{\alpha_1 + (\zeta_{in} + \zeta_g + \frac{\lambda l}{4R})(\frac{\varepsilon a}{a_1})^2}} \tag{7}$$

In which: R – hydraulic radius;

l – length of pressure section;

$\frac{\lambda l}{4R}$ -- streamwise resistance loss factor

ε is calculated using the formula shown in the reference (Li Zhongyi (1995)).

$$\varepsilon = 1\text{-}1.85(s/a)^{0.2} m^{-2.9} \tag{8}$$

Taking ζ_{in} = 0.05, ζ_g = 0.15, α_1= 1, model roughness n = 0.009, we have ε = 0.983, $\frac{\lambda l}{4R} = 0.216, \varphi = 0.879$.

With the above parameters formula (6) can be simplified as follows:

$$H_w = 0.383H+3.64 \text{ (m)} \tag{9}$$

The error range between calculating and testing values of water depth at gate shaft is within 2%.

The pressure on the ceiling of outlet at gate slot is calculated as follows:

$$\frac{p}{\gamma} = H_w - a_1 = 0.383H - 3.36(m) \tag{10}$$

This pressure was taken as reference pressure to calculate flow cavitation number at gate slot or cavitation safety factor K.

As demonstrated by Figure 2 and Figure 3, the cavitation noise frequency spectrum curve and noise energy graph for water flow through mid-outlet and at or above 10kHz, for probe No.4 the maximum ΔSPL ≈ 5dB and the relative noise energy $E/E_1 \approx 2$, for probe No.5 the maximum ΔSPL ≈ 21dB and $E/E_1 \approx 63$. According to experience, incipient cavitation generally occurs when the maximum ΔSPL varies in the range of 5dB~7dB and E/E_1 is about 2. There exist cavitation at both the inlet gate slot and exit diffusion section of mid-outlet. The cavitation noise energy is relatively high at the inlet gate slot and cavitation damage is more liable to occur.

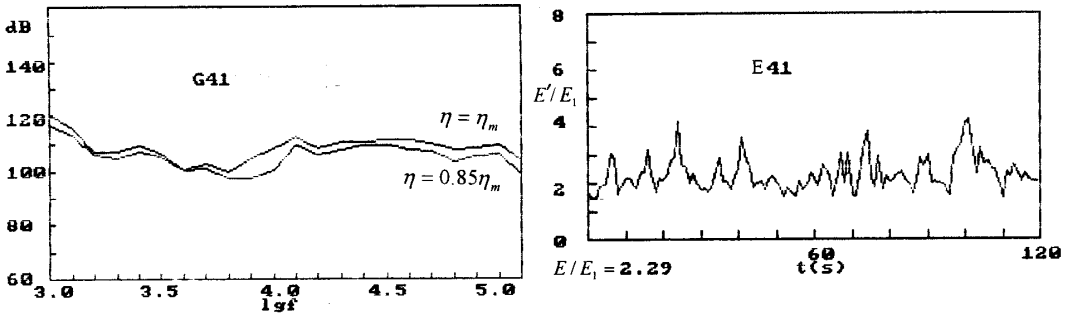

Figure 2 Cavitation noise frequency spectrum curve and noise energy for probe No.4

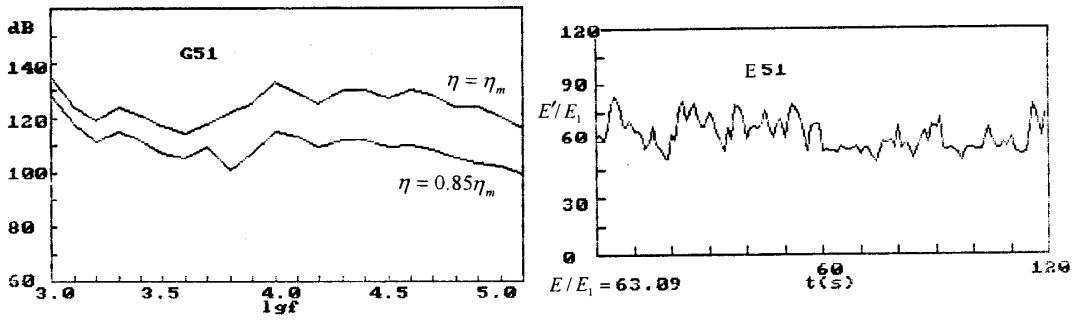

Figure 3 Cavitation noise frequency spectrum curve and noise energy for probe No.5

Figure 4 is the $E/E_1 \sim \eta/\eta_m$ relationship curves for probe No.4 and Figure 5 is for probe No.5. When $\eta = \eta_m$ and at or above 10kHz, $E/E_1 \approx 3.5 \sim 4.0$ from probe No.4 and $\approx 3.0 \sim 3.5$ from probe No.5. In case of incipient cavitation with $E/E_1 \approx 2$, $\eta/\eta_m \approx 0.982$ from probe No.4 and ≈ 0.947 from probe No.5, the cavitation degree K = 0.75 from probe No.4 and = 0.52 from probe No.5. It is usually considered that cavitation occurs when K<0.8. Therefore, cavitation intensity is relatively low at the exit of mid-outlet and fairly high at the inlet gate slot that renders the occurrence of cavitation damage.

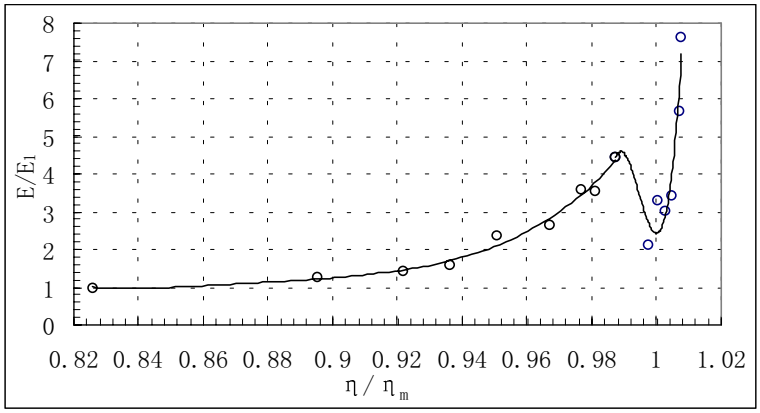

Figure 4 Cavitation characteristics with two sources for probe No.4

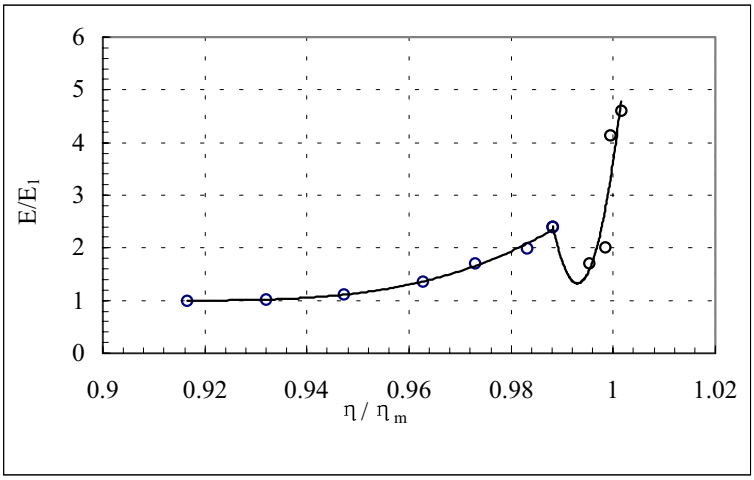

Figure 5 Cavitation characteristics with two sources for probe No.5

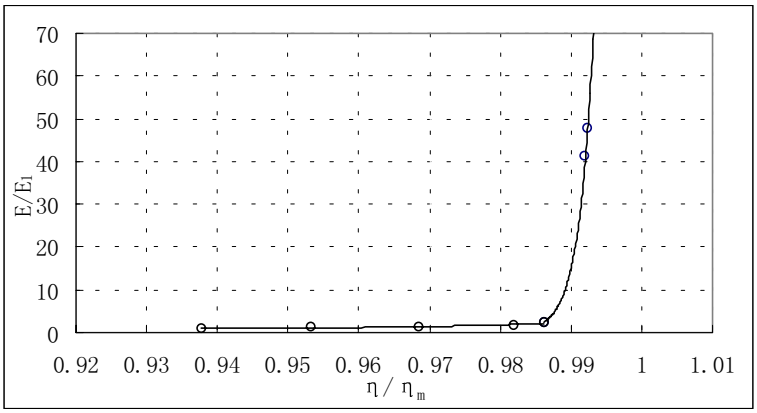

Figure 6 Cavitation characteristics with single source

Two cavitation sources had been found for mid-outlet, respectively at the upper edge of opening wall behind inlet gate slot and the exit diffusion section. Two hydrophones had been set at these two locations. Many times of tests run similar $E/E_1 \sim \eta/\eta_m$ relationship curves. Mutual disturbance of cavitation noise from two sources leads to the relationship curve becoming concave downward and the frequency spectrum sound pressure level decreasing correspondingly when η is close to η_m ($\eta/\eta_m = 1$). With $P_1(t)$ and $P_2(t)$ respectively representing the sound pressure levels of the cavitation sources at gate slot and exit diffusion section, the compound noise sound pressure level (SPL) is calculated with the following formula:

$$P(t) = P_1(t) + P_2(t) = \sum_{i=1}^{\infty} A_i \sin(\omega_i t + \varphi_1) + \sum_{i=1}^{\infty} B_i \sin(\omega_i t + \varphi_2) \tag{11}$$

The total compound SPL may be lower after superposition, since two sound sources have different phases.

In order to further investigate the reason of irregularity of $E/E_1 \sim \eta/\eta_m$ relationship curves, the following work had been carried out. The configuration of the diffusion section at the exit of mid-outlet was modified, aiming at preventing water flow from diffusing in free surface flow section behind the pressure slope, eliminating cavitation resulting from diffusion at the exit, and thereafter avoiding the mutual disturbance of two cavitation sources. For this kind of configuration, $E/E_1 \sim \eta/\eta_m$ relationship curve at the location of hydrophone No.5, the inlet gate slot of mid-outlet, was measured, as shown in Figure 6. This curve is different from that indicated in Figure 4 and Figure 5. Its pattern is in conformity with the general law. E/E_1 increasing monotonously in pace with the rise of η/η_m. It changes greatly when η is close to η_m. Observation demonstrates that cavitation cloud suddenly occurs at the inlet gate slot when $\eta = 0.986\eta_m$, and gradually intensifies along with the rise of η/η_m. These characteristics conform to the measured tendency of curve. Therefore, it was verified that the irregularity of the curve shown in Figure 4 and Figure 5 results from the mutual disturbance of two cavitation sources.

4. Conclusions and Suggestions

Based on the depressurized model test conducted in vacuum chamber for mid-outlet, the following conclusions are drawn.

1). The upper edge of the side wall behind inlet gate slot shall be designed at the same elevation as that in front of gate slot, so as to prevent elevation difference from resulting flow separation, pressure drop and cavitation when water runs through gate slot.

2). The upper edge of sidewall behind the inlet gate slot shall be well rounded in design thus making it possible for water to flow smoothly after running through gate slot.

3). The constriction ratio of mid-outlet exit shall be reduced for the sake of increasing the pressure at closed conduit section.

4). In the curve with single cavitation sources, E/E_1 increasing monotonously in the pace with the rise of η/η_m. It changes greatly when η is close to η_m.

5). Mutual disturbance of cavitation noise from two sources leads to the relationship curve becoming concave downward and the frequency spectrum sound pressure level decreasing correspondingly when η is close to η_m ($\eta/\eta_m = 1$).

6). The discovery may have certain supplementation for the standard of judging the cavitation emergence.

Acknowledgment

The authors express their sincere thanks to Guangxi Hydroelectric Investigation and Design Institute for their great assistances.

References:

Li Zhongyi et al., (February 1997), Hydraulic Model Studies Report on Reconstructing Diversion Tunnel into Flood Discharge Tunnel Adopting Orifice Plates as Energy Dissipation Measures, published in 2nd issue of Hydraulic Engineering.

Li Zhongyi et al., (January 1995), Three Gorge Project: Flood Discharge Deep Outlet Depressurized Model Test Report.

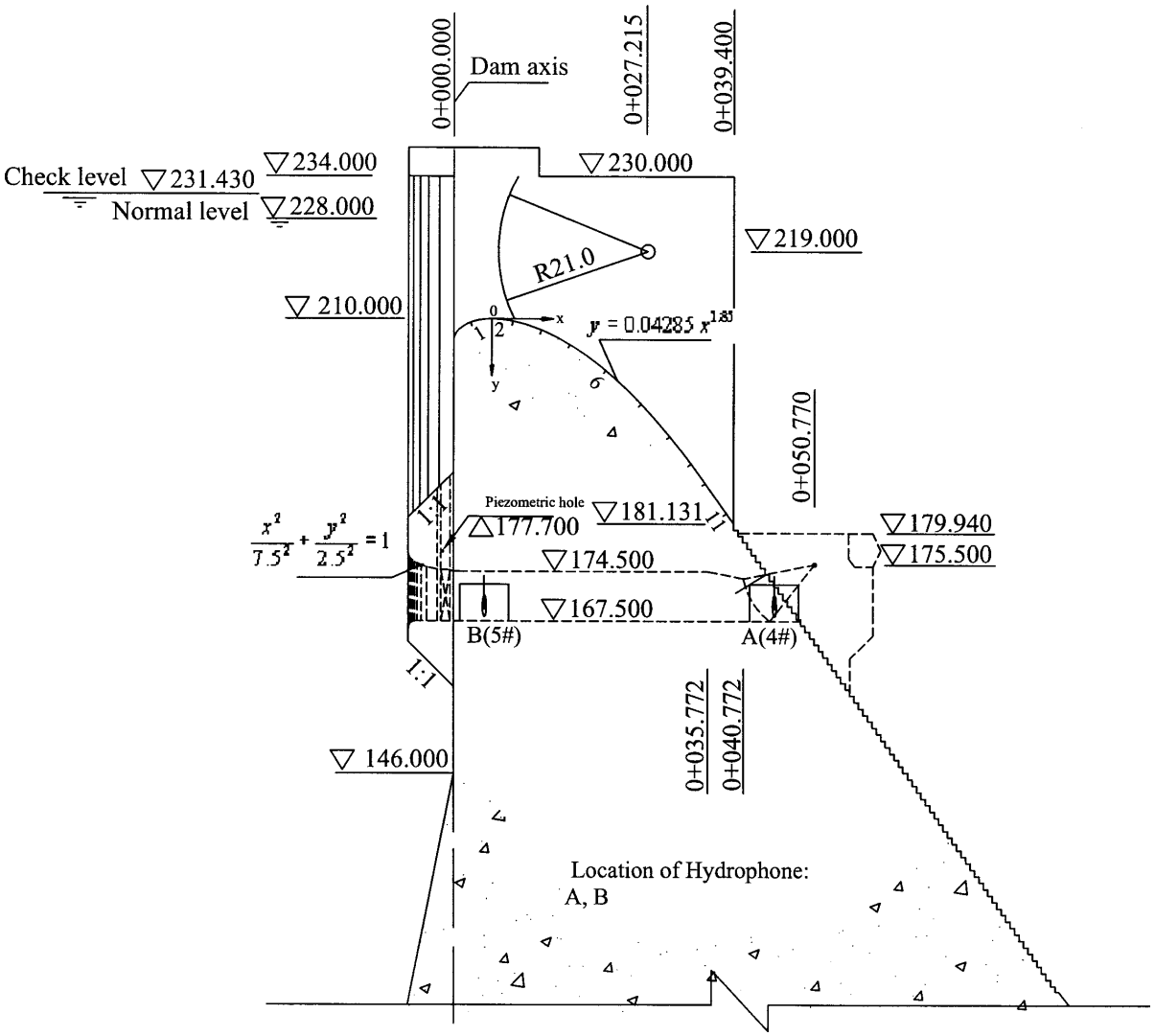

Figure 1 Schematic drawing of layout